Sains Malaysiana 40(1)(2011): 27–33

Effect of $BaAl_2O_4$ Addition on Power Consumption and Oxygen Sensing Response of Er123 Ceramic Rods Utilizing Hot-Spot Phenomenon

(Kesan Penambahan $BaAl_2O_4$ pada Penggunaan Kuasa dan Respon Pengesanan Oksigen pada Rod Seramik Er123 Menggunakan Fenomena Titik Panas)

M. HASSAN, A.K. YAHYA* & T. OKAMOTO

ABSTRACT

In this paper, we report the effect of $BaAl_2O_4$ addition (0-30 wt. %) on power consumption and oxygen sensing response of hot-spots developed on short Er123 ceramic rods of around 12 mm length synthesized using standard solid-state reaction. All the sensor rods showed increase in output current with increasing voltage followed by sudden reduction in output current and appearance of hot spot. After appearance of hot spot, for each rod, output current was observed to decrease gradually with increasing voltage with the slope of the I-V curve gradually approaching zero. Output current after the hot spot formation showed sensitivity to oxygen partial pressure, pO_2 between 1 to 100 kPa. Addition of 30 wt. % $BaAl_2O_4$ reduced the fluctuation of current and increased the sensitivity for pO_2 below 10 kPa. In addition, overshoot current was also reduced and resulted in improvement of response time from around 10 s to 5 s. Our result also showed that minimum power consumption was significantly reduced in the Er123 rods with 30 wt. % $BaAl_2O_4$.

Keywords: Er123; hot spot; oxygen sensor

ABSTRAK

Dalam kertas ini, kami melaporkan kesan penambahan $BaAl_2O_4$ (0-30 wt. %) pada penggunaan kuasa elektrik dan respon pengesanan oksigen di titik panas yang terbentuk pada rod seramik Er123 pendek sekitar 12-mm yang disintesis menggunakan tindak balas keadaan pepejal piawai. Semua rod pengesan menunjukkan pertambahan arus output dengan bertambahnya voltan diikuti pengurangan mendadak arus output dan kemunculan titik panas. Selepas kemunculan titik panas, untuk setiap rod, arus output dicerap mengurang beransur-ansur dengan bertambahnya voltan dengan kecerunan lengkung arus-voltan beransur-ansur mendekati sifar. Arus output selepas pembentukan titik panas menunjukkan kepekaan pada tekanan separa oksigen, pO_2 antara 1 hingga 100 kPa. Penambahan 30 wt. % $BaAl_2O_4$ mengurangkan turun naik arus dan menambahkan kepekaan pada pO_2 di bawah 10 kPa. Tambahan lagi, ayunan lampau arus dikurangkan dan menghasilkan peningkatan masa respon dari sekitar 10 s ke 5 s. Keputusan juga menunjukkan penggunaan kuasa minimum dikurangkan dengan ketara bagi rod Er123 dengan 30 wt. % $BaAl_2O_4$.

Kata kunci: Er123; pengesan oksigen; titik panas

INTRODUCTION

The potential application of $GdBa_2Cu_3O_{7-\delta}$ (Gd123) ceramics utilizing hot spots as oxygen sensing elements was proposed quite recently (Iihama et al. 2009; Okamoto & Takata 2004b). Their suggestion follows earlier observations of formation of oxygen sensitive hot-spots in RE123 (RE=Gd and Sm) ceramic rods (Takata et al. 1999). Upon application of external voltage, the output current was observed to be sensitive to oxygen partial pressure, pO_2 and thus it was suggested as a potential candidate for oxygen sensing in ambient temperature. In contrast to most ambient oxygen sensors (Eguchi et al. 1999; Jiang et al. 2008; Nanda 2008; Ramamoorthy et al. 2003; Schmid et al. 2006; Warburton et al. 2001), the design of the hot-spot based sensors is in the form of a simple thin rod which can be easily fabricated and reproduced for large scale industrial applications. Besides being external-heater free, the sensor also uses a simple sensing system based on magnitude of output current.

Formation of hot spot on Gd123 and Sm123 rods when a high enough voltage is applied was suggested to be related to the positive temperature coefficient of resistivity (PTCR) behaviour of the ceramics where large increase in resistivity takes place above 400°C (Takata et al. 1999; Okamoto & Takata 2004b). The hot spot is triggered as a result of large voltage drop concentrated across a point with the highest resistivity due to microstructural defect. As heating progresses at the point, temperature increases and this in turn increases resistivity of the heated point further until a glowing spot is formed. After appearance of a hot spot, the output current approaches a constant value and a plateau is formed with further increase in applied voltage. The oxygen sensing properties were suggested to be due to absorption of oxygen gas by the hot spot before

dissociating into oxide ions and holes. The number of oxide ions and holes increases with oxygen partial pressure causing an increase in conductivity and sensor output current (Takata et al. 1999).

The temperature of the hot spot was reported to reach as high as 940°C (Takata et al. 1999) which is close to the melting temperature of RE123 materials and is detrimental to the durability of the sensor rods. Several study were conducted to increase the durability of RE123 sensor rods by addition with secondary materials such as $BaAl_2O_4$ (Okamoto and Takata 2004a), $BaZrO_3$ (Tsutai et al. 2004) and Gd_2BaCuO_5 (Okamoto et al. 2006). Interestingly, addition of the secondary phase also showed improvement of stability and repeatability of sensor output current (Okamoto & Takata 2004a). However, all the reports were based on 30 mm long rods and to our knowledge there is no similar study on effects of secondary additions on output current in much shorter rods. Shorter rods are not only expected to reduce power consumption due to its lower voltage applied (Okamoto & Takata 2001) but it may also show slightly different oxygen sensing properties due to slightly different temperature distribution between its two ends compared to longer rods. On the other hand, previous study on oxygen desorption by heated hot-spot free RE123 ceramics showed that the activation energy of oxygen ions was higher for RE123 rods with smaller ionic radius of RE^{3+} (Buchgeister et al. 1991) which may alter its resistivity versus temperature behaviour. Since for RE123 sensor rods only a small area of the rod glows into a hot spot while the rest remains normal, the output current response of the normal areas is expected to be largely influenced by ionic radius of RE^{3+} and should result in differences in oxygen sensing properties of 123 rods with different RE^{3+}. As such, it is interesting to study the sensing properties of other RE123 materials not previously reported such as Er123 with addition of an additive such as $BaAl_2O_4$.

In this paper, we report the study of oxygen sensing behaviour of hot-spot based Er123 short rods with addition of $BaAl_2O_4$ between 0-30 wt. %. Results of structural and microstructural investigation using Powder X-ray Diffraction (XRD) and scanning electron microscope (SEM), respectively, are analyzed and discussed. Addition of $BaAl_2O_4$ in the short Er123 sensor rods was found to reduce power consumption by around 42% and also enhanced sensitivity of the sensor for low oxygen partial pressure.

Experimental Details

Bulk Er123 sample was synthesized from high purity (≥99.95%) Er_2O_3, $BaCO_3$ and CuO powders using the standard solid-state reaction method. Appropriate amounts of the powders were mixed and ground in an agate mortar. The powders were then calcined in a box furnace at 900°C for 48 hours with several intermittent grindings. The calcined powders were reground and pressed into 13 mm-diameter pellets before sintering at 900°C for 24 hours in a box furnace followed by slow cooling to room temperature. The Er123 pellets were then reground to obtain fine Er123 powder. $BaAl_2O_4$ powder was also prepared by using the standard solid-state reaction from Al_2O_3 and $BaCO_3$ powders. The appropriate amounts of powders were mixed and ground in an agate mortar before calcination in a box furnace at 1200°C for 48 h with several intermittent grindings. The Er123 powder was mixed with 0, 5, 10, 15 and 30 wt. % $BaAl_2O_4$ powder and ground before pressed into 13-mm diameter pellets and sintered at 900°C for 24 h in box furnace. The composite pellets were fabricated into sensor rods by cutting them into short rods of approximate dimension 12 mm × 0.65 mm × 0.65 mm. Powder X-ray Diffraction (XRD) analyses using Rigaku model D/MAX 2000 PC with Cu-K_α radiation source was used to confirm the phase structures formed during the preparation process. Microstructural investigation and elemental distribution of the samples were investigated using JEOL model JSM-6360LA scanning electron microscope (SEM) with Energy dispersive X-ray spectrometer (EDX).

Electrical characterization was performed using the standard four-point-probe method with the distance between voltage electrodes maintained at around 9 mm. Voltage between the electrodes was supplied by an Agilent model 6575A DC power supply. The current and voltage through the sensor were measured using Keithley multimeters models 2000 and 197A, respectively. PTCR behaviour of the composite rods was investigated by heating them in a box furnace from 30 to 900°C at a rate of 7.5°C min^{-1}. Response current versus voltage (I-V) and time characterizations of the sensors were conducted in a chamber with oxygen partial pressure, pO_2 controlled by adjusting the flow rate of oxygen and nitrogen gas, respectively. The experimental setup is schematically shown in Figure 1.

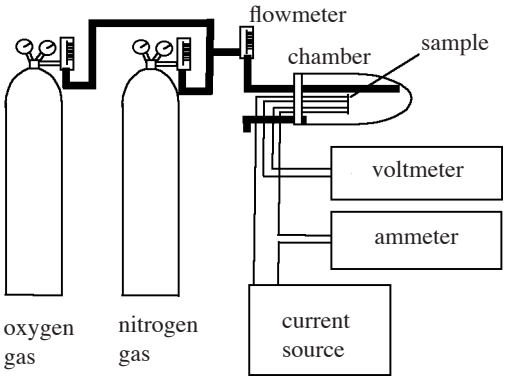

FIGURE 1. Schematic diagram of the experimental setup for measurement of sensor output current under different oxygen partial pressures

Results and Discussion

XRD analysis showed all samples consist of 123 orthorhombic structure with space group *Pmmm*. Figure 2 shows XRD patterns for Er123 with 0 and 30 wt. % $BaAl_2O_4$. For undoped Er123, the calculated lattice parameters of

the single phase structure are a = 3.814 Å, b = 3.882 Å and c = 11.675 Å, respectively. Existence of $BaAl_2O_4$ as a secondary phase was clearly shown in the XRD pattern for Er123 with 30 wt. % $BaAl_2O_4$ (Figure 2).

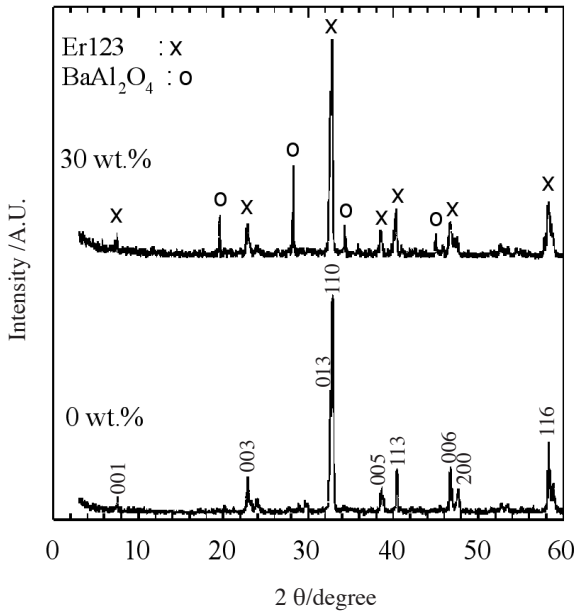

FIGURE 2. XRD patterns of Er123 composites with 0 and 30 wt. % $BaAl_2O_4$

SEM for all samples showed irregular shaped grains in addition to existence of voids and pores. There is also a noticeable reduction in porosity with increasing amount of $BaAl_2O_4$. Figure 3 shows SEM images for fractured surface of the Er123 composite samples with 0, 5, 15 and 30 wt.% $BaAl_2O_4$ and EDS maps of Cu and Al for same spot of SEM images of samples with 5 and 15 wt.% $BaAl_2O_4$. In the elemental maps, the white area indicates a high concentration of the elements. Cu and Al were considered to show the distribution of Er123 and $BaAl_2O_4$, respectively. The images and maps indicate that the samples had porous microstructures composed of grains of both Er123 and $BaAl_2O_4$. The images also show the coating effect at Er123 grains by $BaAl_2O_4$ in sample with 15 wt. % $BaAl_2O_4$ and the effect increased in sample with 30 wt. % $BaAl_2O_4$.

Figure 4 shows sample resistivity normalized to resistivity value at furnace temperature of 900°C versus furnace temperature for samples with 0, 15 and 30 wt. % $BaAl_2O_4$ and the inset table shows resistivity at 30°C and 900°C for the samples. The results show that addition of $BaAl_2O_4$ increased resistivity of the composite more at the temperature region below 540°C compared to the higher temperature region. The 30 wt. % $BaAl_2O_4$ sample showed strong semiconductor-like behaviour compared to other samples at the lower temperature region. Above 540°C all samples showed clear PTCR behavior where resistivity sharply increase with increasing temperature.

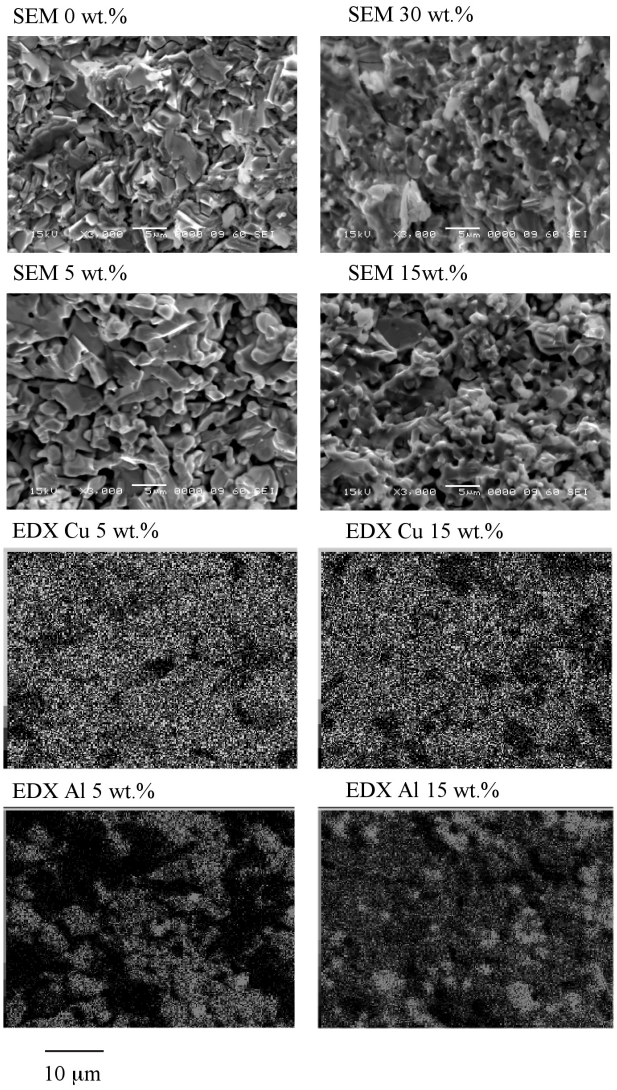

FIGURE 3. SEM images for fractured surface of samples with 0, 5, 15 and 30 wt. % $BaAl_2O_4$ and EDX maps of Cu and Al for fractured surface of samples with 5 and 15 wt. % $BaAl_2O_4$

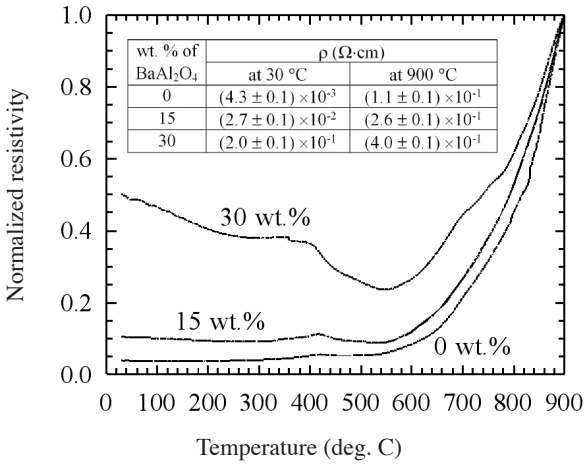

FIGURE 4. Normalized resistivity (R(T)/R(900°C)) versus furnace temperature for sample with 0, 15 and 30 wt. % $BaAl_2O_4$. The inset table shows values of resistivity at furnace temperature 30°C and 900°C for 0, 15 and 30 wt.% $BaAl_2O_4$

Figure 5 shows the current-voltage characteristics of the composite ceramic rods with various $BaAl_2O_4$ contents in oxygen partial pressure of 21 kPa (open air). All samples show increase in output current with increasing voltage until the current reached its maximum. The slope of curves before peak current, I_p was reached at respective applied voltage, V_p, was observed to decrease with increasing $BaAl_2O_4$ indicating gradual increase in sample resistivity. For all rods, the drop in output current after I_p was accompanied by appearance of a dark-red hot spot. For the 0-10 wt. % $BaAl_2O_4$ rod, after I_p the output current gradually dropped but for higher doping the drop becomes lesser. In general, the current-voltage characteristics for all the rods also agree with the previous study reported by Okamoto and Takata (2001) for short rods. Further increase of applied voltage caused output current to decrease and the glow of the hot spot becoming brighter and its colour changed from reddish to orange.

For comparison of power consumption between rods, minimum power consumption (P_c) is defined from product of minimum working voltage (V_c) and its output current in the respective current-voltage characteristic curve of the sensor. V_c is in turn defined as the minimum voltage when a constant current plateau (I_c) with a variation of less than 0.01 A/V is achieved. Beyond V_c, the length of the hot spot started to increase and output current (I_c) became a plateau. Figure 6 shows the photograph of the hot spot in Er123 with 30 wt. % $BaAl_2O_4$ just as the length of hot spot started to increase. The length of hot spot just before breakage of the rod was also observed to increase with amount of $BaAl_2O_4$.

Table 1 shows I_p, V_p, I_c, V_c and P_c for each sensor rod. Addition of $BaAl_2O_4$ increased V_p and V_c but decreased I_p and I_c. In general, addition of $BaAl_2O_4$ from 0 wt. % to 30 wt. % increased P_c from 1.03 W to 1.16 W. From previous report, the P_c value estimated from I-V curves for Gd123 with addition of $BaAl_2O_4$ between 0 to 50 mol% (26 wt. %) were between 1.4 W and 2.7 W (Okamoto & Takata 2004a), and the lowest estimated P_c after $BaAl_2O_4$ addition is around 2 W (addition with 10 mol% $BaAl_2O_4$) (Okamoto & Takata 2004a). As such, compared to the previous work, P_c for the shorter undoped Er123 sensor rod showed power consumption of only 1.03 W which is a reduction of more than 36% compared to the value

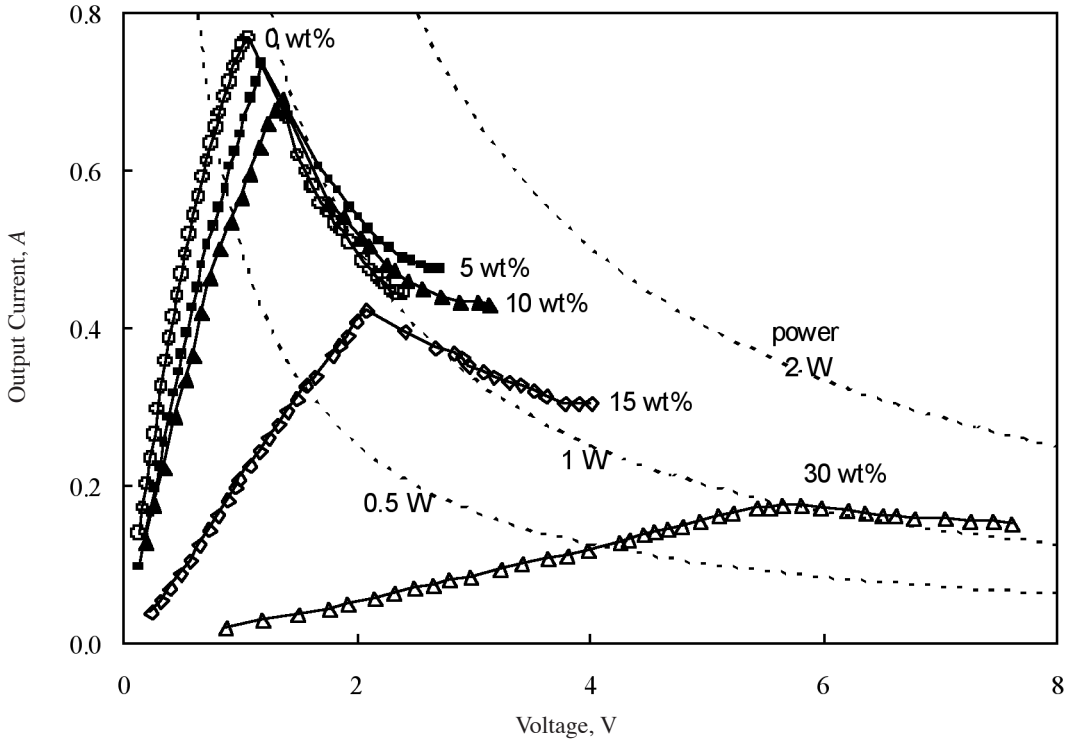

FIGURE 5. Current-voltage characteristics of Er123 with addition of 0, 5, 10, 15 and 30 wt. % $BaAl_2O_4$. The dotted curves are just as a guide to the eye to show electrical power consumption of 0.5, 1 and 2 Watts

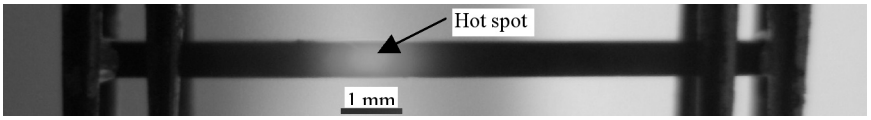

FIGURE 6. Photograph of a hot spot in Er123 with 30 wt. % $BaAl_2O_4$ after applying a dc voltage of 7.2 V

TABLE 1. I_p, V_p, I_c, V_c and P_c values for Er123 sensor rods with 0, 5, 10, 15 and 30 wt% $BaAl_2O_4$

$BaAl_2O_4$ (wt. %)	V_p (V±0.01 V)	I_p (A±0.01 A)	V_c (V±0.01 V)	I_c (A±0.01 A)	P_c (W)
0	1.07	0.77	2.29	0.45	1.03
5	1.18	0.74	2.62	0.47	1.23
10	1.34	0.69	2.87	0.43	1.23
15	2.07	0.42	3.77	0.31	1.17
30	5.64	0.18	7.24	0.16	1.16

of 1.4 W reported for the longer Gd123 rod. Addition of 30 wt. % $BaAl_2O_4$ in Er123 only increased P_c to 1.16 W, an increase of 13% from that of undoped Er123. Interestingly, further addition of $BaAl_2O_4$ from 5 to 30 wt. % in short rod Er123 also reduced P_c from 1.23 to 1.16 W. By comparing the lowest P_c between the studies for all data with $BaAl_2O_4$ addition, using short rod of Er123 with 30 wt. % $BaAl_2O_4$ gives lower P_c (1.16 W) compared to using longer rod Gd123 with 10 mol% $BaAl_2O_4$ (2 W) by reduction factor of around 42%.

Figure 7 shows the output current response in 0 and 30 wt. % $BaAl_2O_4$ after applying alternate pO_2 (1-100-1 kPa). It was observed that rod with 0 wt.% $BaAl_2O_4$ showed a larger output current in response to the change in pO_2 compared to the rod with 30 wt. % $BaAl_2O_4$. However, the former showed a large overshoot current on the rising edge whose magnitude was around 30% of the average current response level. Interestingly, addition of 30 wt. % $BaAl_2O_4$ suppressed the overshoot current and produced a more stable response current at 100 kPa. These also results in a large improvement in sensing response time from around 10 s for the undoped Er123 rod to 5 s for the 30 wt. % $BaAl_2O_4$ added Er123 rod.

Figure 8 shows the output current response versus pO_2 in Er123 rods with 0 and 30 wt. % $BaAl_2O_4$ under increasing pO_2 from 1 to 100 kPa. To show the sensitive response of sensor rod with increasing pO_2 from p_1 to p_2, average sensitivity is defined as:

$$S = \frac{(i_2 - i_1)/i_1}{P_2 - p_1}, \quad (1)$$

where i_1 and i_2 are the output currents at p_1 and p_2, respectively. Based on the equation the average sensitivity of the sensor rods are calculated and plotted in Figure 9. In the figure, it can be observed that for partial pressure below 10 kPa a significant enhancement in oxygen sensitivity was observed in the 30 wt. % $BaAl_2O_4$ added rod compared to the undoped rod. However, between 10 and 100 kPa, sensitivity of the 30 wt. % $BaAl_2O_4$ added rod is lower, which resulted in reduction of the average sensitivity between 1 to 100 kPa. This explains the smaller response current observed for the Er123 rod with 30 wt. % $BaAl_2O_4$ as shown in Figure 7.

Conductivity in hot-spot based RE123 rods has been suggested as predominantly due to oxide ions and holes resulting from dissociation of absorbed oxygen at the hot spot and based on mass action law, the conductivity, σ is related to oxygen concentration (Takata et al. 1999) and is given by

$$\sigma \propto pO_2^{1/6}. \quad (2)$$

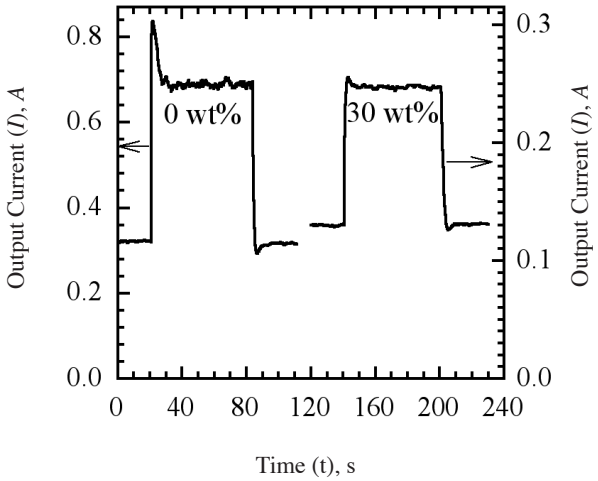

FIGURE 7. Output current response in 0 and 30 wt. % $BaAl_2O_4$ after applying alternate pO_2 (1-100-1 kPa)

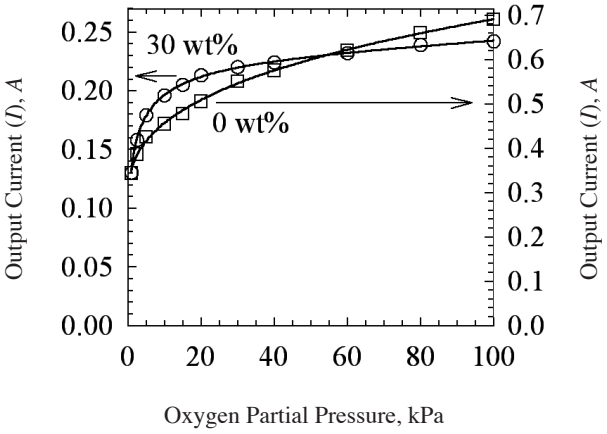

FIGURE 8. Output current response versus pO_2 for Er123 sensor rods with addition of 0 wt. % $BaAl_2O_4$ and 30 wt. % $BaAl_2O_4$

Since conductivity is proportional to output current, output current is proportional to $pO_2^{1/6}$. Figure 10 shows log of output current versus log of oxygen partial pressure for Er123 sensor rods with 0 and 30 wt. % $BaAl_2O_4$. The solid line based on equation $I = k\ pO_2^{1/6}$ where k is a constant is drawn as a comparison. From the figure, it can be seen that for rod with 0 wt. % $BaAl_2O_4$ the output current showed very good proportional relation to $pO_2^{1/6}$ from 10 to 100 kPa but slightly deviates from the calculated curve for pO_2 lower than 10 kPa. This is in contrast to Sm123 (Takata et al. 1999) and Gd123 (Okamoto and Takata 2004a) which showed good agreement with the calculated curve at as low as 0.5% and 1% pO_2, respectively. These differences may be due to the ionic size of the RE^{3+} ion used for the sensor rods. RE^{3+} ionic size is known to affect internal pressure of the unit cell and lead to differences in oxygen uptake response (Plackowski et al. 1998). On the other hand and for the Er123 rod with 30 wt. % $BaAl_2O_4$ the conductivity showed good proportional relation to $pO_2^{1/6}$ below 10 kPa but deviates for higher partial pressures.

Based on resistivity behaviour below 540°C (Figure 4) it is clear that the heating behaviour for Er123 rod with 30 wt.% $BaAl_2O_4$ is very different from the 123 rods with 0 and 15 wt.% $BaAl_2O_4$. At lower temperature regions the rod with 30 wt.% $BaAl_2O_4$ is expected to draw larger voltage drop and higher joule heating compared to the other rods. Since the colder regions are near the terminals larger joule heating takes place for the 30 wt.% $BaAl_2O_4$ and caused larger power loss by heat conduction to the terminal. This is suggested as the main factor that increases the amount of minimum power consumption (P_c) for rods with higher amount of $BaAl_2O_4$ (Table 1).

The overshoot current observed for the undoped Er123 rod (Figure 7) is suggested to be due to drop in output current from the initial response to oxygen partial pressure of 100 kPa as a result of increase in temperature of the hot spot. When pO_2 increased from 1 to 100 kPa, oxygen gas diffused into the hot spot caused a sharp increased in output current but this is immediately followed by increase in Joule heating which increased the temperature of the rod (Takata et al. 1999). As a result, resistivity increased and caused the current to drop until a stable temperature is reached. The reduction in overshoot current for the Er123 rod with 30 wt.% $BaAl_2O_4$ indicates some form of accelerated stabilization effect on temperature of the rod as a result of addition of the secondary phase.

For rod with 0 wt.% $BaAl_2O_4$, the deviation of output current from the theoretical curve based on Eq. 2 for pO_2 lower than 10 kPa (Figure 10) indicates that due to the low oxygen partial pressure the concentration of oxide ions and holes formed from dissociation of absorbed oxygen at the hot spot was much smaller and was no longer the main charge carrier in the Er123 rod. As such, with the reduction of oxide ions and holes, conductivity of the Er123 rod at this level is suggested to depend also on intrinsic carriers.

For rod with 30 wt.% $BaAl_2O_4$, at pO_2 higher than 10 kPa, the deviation of output current was not expected and it may due to the effect of current tunnelling through $BaAl_2O_4$ layers in between grains. It is suggested that at low amount of $BaAl_2O_4$ current was able to percolate through Er123 grains and interfaces but at 30 wt.% $BaAl_2O_4$ the secondary phase coated Er123 grains and conduction was mainly due to tunnelling current.

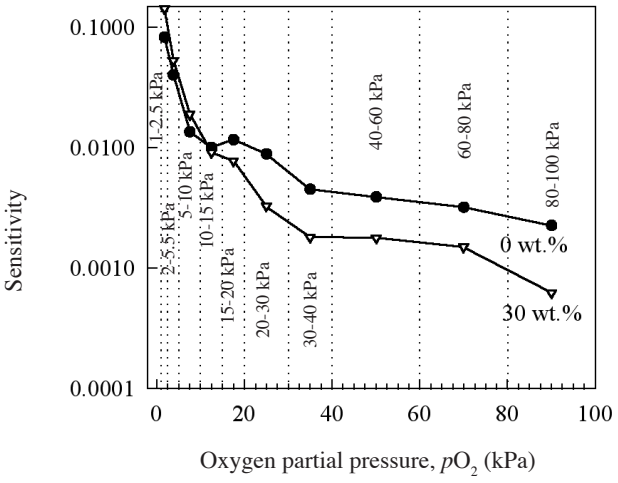

FIGURE 9. Average sensitivity versus oxygen partial pressure, pO_2 for Er123 rods with 0 and 30 wt% $BaAl_2O_4$

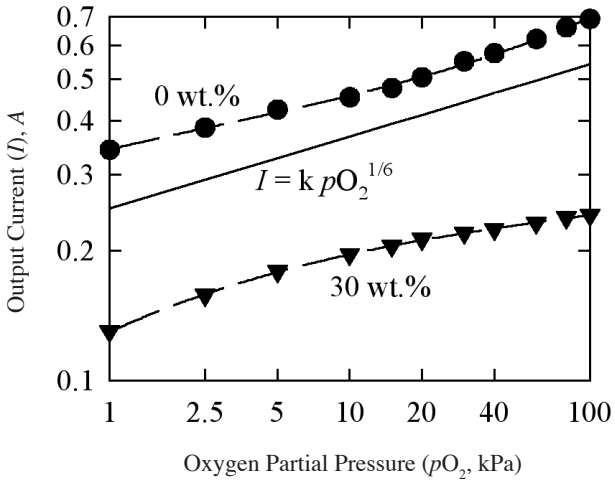

FIGURE 10. Log of output current versus log of oxygen partial pressure for Er123 sensor rods with 0 and 30 wt. % $BaAl_2O_4$. The solid line is based on equation $I = k\ pO_2^{1/6}$ and is drawn as a comparison guide to the eye

CONCLUSION

Short rods of $BaAl_2O_4$-added Er123 ceramic oxygen sensor were successfully synthesized and fabricated. From I-V characterization, by using short rod of Er123 with 30 wt.% $BaAl_2O_4$, minimum power consumption was lowered by reduction factor of at least around 42% compared to using longer rod of Gd123 with any amount of $BaAl_2O_4$ addition from previous study. Addition of $BaAl_2O_4$ also reduced the

fluctuation of current and increased the sensitivity below 10 kPa. In addition, addition of $BaAl_2O_4$ reduced the overshoot current which resulted in lowering the response time from around 10 to 5 s.

ACKNOWLEDGEMENTS

This research has been supported by the Malaysian Ministry of Science, Technology and Innovation under e-science grant no. 03-01-01-SF0001.

REFERENCES

Buchgeister, M.,Herzog, P., Hosseini, S.M., Kopitzki, K. & Wagener, D. 1991. Oxygen evolution from $ABa_2Cu_3O_{7-\delta}$ high-Tc superconductors with A=Yb, Er, Y, Gd, Eu, Sm, Nd and La. *Physica C* 178(1-3): 105-109.

Eguchi, Tomoyasu, Soichiro Suda, Hiroko Amasaki, Jun Kuwano & Yasukazu Saito. 1999. Optimum design for the sensing electrode mixtures of $PbSnF_4$-based oxygen sensors for fast response at ambient temperature. *Solid State Ionics* 121(1-4): 235-243.

Nanda, G.P. 2008. Measurement of gas concentrations: oxygen, carbon dioxide, nitrogen, nitrous oxide and volatile anaesthetic agents. *Anaesthesia & Intensive Care Medicine* 9(12): 559-563.

Iihama, Kazufumi, Yuichiro Kuroki, Tomoichiro Okamoto, and Masasuke Takata. 2009. Characteristics of hot spot oxygen sensor using $GdBa_2Cu_3O_{7-\delta}$-CuO composite ceramics. *Current Applied Physics* 9 (3, Supplement 1): S167-S169.

Jiang, Jinjun, Lei Gao, Wei Zhong, Shen Meng, Ben Yong, Yuanlin Song, Xiangdong Wang & Chunxue Bai. 2008. Development of fiber optic fluorescence oxygen sensor in both in vitro and in vivo systems. *Respiratory Physiology & Neurobiology* 161(2): 160-166.

Okamoto, T., Iihama, K. & Takata, M. 2006. Hot spot oxygen sensor using $GdBa_2Cu_3O_{7-\delta}$-based composite ceramics. *Advanced Materials Research* 11-12: 137-140.

Okamoto, T. & Takata, M. 2001. Effect of Relative Density & Length of $GdBa_2Cu_3O_{7-\delta}$ Ceramic Rod on Hot Spot Appearance. *Transactions of the materials Research Society of Japan* 26 (1): 19-22.

Okamoto, T. & Takata, M. 2004a. Characteristics of oxygen sensor exploiting the hot spot in $BaAl_2O_4$-added $GdBa_2Cu_3O_{7-\delta}$ composite ceramic rod. *Journal of the Ceramic Society of Japan* 112-1: S567-S571.

Okamoto, T. & Takata, M. 2004b. Development of functional devices using hot spot in $GdBa_2Cu_3O_{7-\delta}$-based composite ceramics. *Ceramics International* 30(7): 1569-1574.

Plackowski, T., Sulkowski, C., Wlosewicz, D. & Wnuk, J. 1998. Effect of the RE^{3+} ionic size on the $REBa_2Cu_3O_{7-\delta}$ ceramics oxygenated at 250 bar. *Physica C* 300(3-4): 184-190.

Ramamoorthy, R.,Dutta, P.K. & Akbar, S.A. 2003. Oxygen sensors: Materials, methods, designs and applications. *Journal of Materials Science* 38(21): 4271-4282.

Schmid, U., Seidel, H., Mueller, G. & Becker Th. 2006. Theoretical considerations on the design of a miniaturised paramagnetic oxygen sensor. *Sensors and Actuators B* 116(1-2): 213-220.

Takata, M., Noguchi, Y., Kurihara, Y., Okamoto, T. & Huybrechts, B. 1999. Novel oxygen sensor using hot spot on ceramic rod. *Bulletin of Materials Science* 22(3): 593-600.

Tsutai, Y., Okamoto, T., Kawamoto, A. & Takata, M. 2004. Hot spot in $GdBa_2Cu_3O_{7-\delta}$-$BaZrO_3$. *J. Ceram. Soc. Japan* 112-1: S599-S601.

Warburton, Richard, P., Scott Sawtelle, R., Adam Watson, & Annie Q. Wang. 2001. Failure prediction for a galvanic oxygen sensor. *Sensors and Actuators B* 72(3): 197-203.

M. Hassan & A.K. Yahya*
Faculty of Applied Sciences
Universiti Teknologi MARA
Shah Alam, Selangor D.E.
Malaysia

T. Okamoto
Department of Electrical Engineering
Nagaoka University of Technology, Niigata
Japan

*Corresponding author; email: ahmad191@salam.uitm.edu.my

Received: 7 December 2009
Accepted: 13 July 2010